

Alizarin complexone: an interesting ligand for designing TiO₂-hybrid nanostructures†

Cite this: *New J. Chem.*, 2013, **37**, 969

Yesica Di Iorio,^a Rodrigo Parra,^b Konrad Szaciłowski^{cd} and Maria A. Grela^{*a}

Herein we report the characterization and photoelectrochemical behavior of nanocrystalline TiO₂ films modified with some alizarin derivatives. Particularly, alizarin complexone (3-[*N,N*-bis(carboxymethyl)-aminomethyl]-1,2-dihydroxyanthraquinone) and its Fe(II) and Fe(III) metal complexes have been examined. Based on UV-Visible and Raman spectroscopic studies we proposed that AC forms a tridentate complex with titanium dioxide involving the 2-OH and (methylimino) diacetate groups, while Fe(II) and Fe(III) AC-complexes bind to titanium dioxide through the carbonyl (C=O) and hydroxyl (OH) groups at the 1,9 positions of the alizarin framework. These findings allow the design of different nanostructures with diverse photoelectrochemical behavior. Analysis of the *j*-*V* curves reveals a sign reversal at −90 mV and −100 mV upon the excitation of AC@TiO₂ and [Fe^{III}AC]@TiO₂ photoelectrodes, respectively, whereas [Fe^{II}AC]@TiO₂ displays only anodic photocurrents. A description involving both electronic and geometric factors to account for these differences is proposed.

Received (in Montpellier, France)
29th October 2012,
Accepted 11th January 2013

DOI: 10.1039/c3nj40979a

www.rsc.org/njc

Introduction

Hybrid systems composed of organic molecules adsorbed on semiconductor nanoparticles provide interesting platforms for the development of memory devices, logic gates and for the design of materials for information processing, and sensing.^{1–10} Particularly, recent theoretical studies indicate that polycyclic aromatic systems are well suited surface modifiers for titanium dioxide and other oxide phases.¹¹ It has recently been shown that the photoinduced current sign in ligand-modified TiO₂ electrodes can be modulated by changing the excitation wavelength^{12,13} and by chemical¹⁴ or electrical inputs.^{13,15} In this context, the phenomenon commonly referred to as photoelectrochemical photocurrent switching, PEPS, makes reference to the photocurrent sign-reversal induced by an applied potential.^{1,15} This behavior was previously observed for nanostructured electrodes modified with carminic acid¹⁵ and 1,2-dihydroxy-9,10-anthraquinone (alizarin, A).¹⁶

Alizarin forms a strong chelate with titanium dioxide nanoparticles apparently involving the 1,2 hydroxyl groups.^{16–19} On the other hand, this molecule bears two redox-active quinoid fragments, the 9,10-dioxo and the 1,2-catechol-like fragment which may act as electron acceptor and electron-donor groups, respectively.^{16–19} We have recently shown that these properties are necessary to account for the development of anodic and cathodic photocurrents under visible irradiation.¹⁶

Here we focused on 3-[*N,N*-bis(carboxymethyl)-aminomethyl]-1,2-dihydroxy-anthraquinone (alizarin complexone, hereafter mentioned as AC) as a TiO₂-ligand to examine the PEPS effect. The interest in this system lies in the retention of the basic framework of A, adding two carboxylate groups that afford site possibilities for metal chelation.²⁰ It has been demonstrated that AC forms highly stable tridentate colored complexes with different metals, M, hereafter designated M-AC.^{21–26} Various of these complexes have been studied and characterized.^{23,27} The binding of the metal to AC is believed to occur through the (methylimino) diacetate and the 2-OH groups of alizarin complexone. It has been established that M-AC stability may be accounted by M attachment to the EDTA-derived moiety of the alizarin frame. Besides, the formation of an additional bond between M and the oxygen atom at position 2 explains the color change observed upon formation of the M-AC complex.

In this paper we show that the existence of multiple moieties in alizarin complexone opens up new possibilities of interaction with the semiconductor, and allows the design of combined

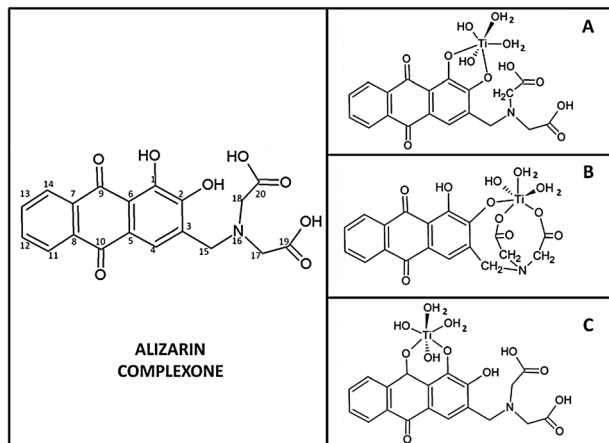
^a Departamento de Química, Universidad Nacional de Mar del Plata, Funes 3350, B7602AYL Mar del Plata, Argentina. E-mail: magrela@mdp.edu.ar

^b Instituto de Investigaciones en Ciencia y Tecnología de Materiales (INTEMA, UNMdP-CONICET), J.B. Justo 4302, B7608FDQ Mar del Plata, Argentina

^c AGH Akademia Górniczo-Hutnicza, Wydział Metali Nieżelaznych, al. A. Mickiewicza 30, 30-059 Kraków, Poland

^d Wydział Chemii, Uniwersytet Jagielloński, ul. R. Ingardena 3, 30-060 Kraków, Poland

† Electronic supplementary information (ESI) available. See DOI: 10.1039/c3nj40979a



Scheme 1 Left: chemical structure of alizarin complexone (AC). Right: simplified models showing possible ways of interaction of titanium dioxide with the ligand: through the enediol group (A); the 2-OH and the (methylimino) diacetate adjacent moiety (B); and the 9-carbonyl and 1-OH groups (C).

M-AC@TiO₂ nanostructures with distinctive photoelectrochemical behaviour. Possible modes of interaction between AC and the TiO₂ surface are briefly outlined in Scheme 1.

Experimental section

Materials

3-[N,N-Bis(carboxymethyl)-aminomethyl]-1,2-di-hydroxyanthraquinone (alizarin complexone) and titanium isopropoxide Ti[OCH(CH₃)₂]₄ were of the highest purity available and used as received. Quinizarin (1,4-dihydroxy-anthraquinone, Q), iron(II) sulfate heptahydrate and iron(III) nitrate nonahydrate were purchased from Sigma-Aldrich and Merck, respectively, and used as received.

KCr(NH₃)₂(NCS)₄ was prepared from the Reinecke salt²⁸ (Aldrich) and recrystallized from warm water as described in ref. 28. Aqueous solutions were prepared with deionized ultrapure water of resistivity < 18.0 MΩ cm. TiO₂ films were prepared from a commercially available TiO₂ paste based on nanosized particles (Solaronix, Ti-nanoxide T; average diameter, *d* = 13 nm).

Methods

AC chemisorption was analyzed both in a TiO₂ nanoparticle solution and in nanostructured-semiconductor films.

Colloidal TiO₂ was prepared by controlled acid hydrolysis of titanium tetraisopropoxide following standard procedures.^{17,18} Briefly, Ti[OCH(CH₃)₂]₄ (1 mL) was dissolved in 2-propanol (20 mL) and slowly added to an aqueous HClO₄ solution (200 mL, pH 1.5) maintained at 1 °C. The solution was continuously stirred in the dark, for 48–72 hours to promote aging and for a more stable and uniform particle size distribution.

Nanoporous TiO₂ films of 1 cm² of geometric area, unless specified, were prepared on transparent conducting glass slides (indium tin oxide, surface resistivity: 15–25 Ω square^{−1}). Briefly, a drop of the Ti-nanoxide T sol was placed at near the end of the electrode. By capillarity action, when the drop is touched with a

microscope slide it slips all along its border. Using Scotch tape as a frame and spacer, a thin uniform film on the surface of the conductive substrate was formed by raking off the excess of the colloidal paste. The films were then dried at room temperature, heated at 400 °C (at 5 °C min^{−1}) and then left at this temperature for two hours.

Nanostructured modified electrodes were obtained by dipping the semiconductor electrodes in ethanol solutions containing the ligand for 48 hours in a dark N₂-atmosphere under agitation. We used 4.5 mM AC, 0.5 mM [Fe^{II}-AC], 0.5 mM [Fe^{III}-AC] and 10 mM Q solutions to obtain AC@TiO₂, [Fe^{II}AC]@TiO₂, [Fe^{III}AC]@TiO₂, and Q@TiO₂ films, respectively.

Raman spectra were measured with a Renishaw inVia micro-Raman instrument using a 514 nm Ar-ion laser line (50 mW nominal power) as the excitation source with a diffraction grating of 2400 lines per nm. The measurements were performed by dripping the nanoparticle suspension on a glass slide.

The UV-Vis spectra of the films were recorded with an integrating sphere accessory (Hitachi U-3210 model, 60 mm sphere diameter, opening ratio: 7.8%).

The photoelectrochemical studies were carried out in a 20 mL square single-compartment, three-electrode cell, using a commercial potentiostat/galvanostat, TEQ-04, Argentina, interfaced to a personal computer. Ligand modified nanocrystalline TiO₂ films were used as working electrodes. In addition, Ag/AgCl and a Pt foil served as reference and counter electrodes, respectively. The working electrode was illuminated from the back-side (light first hits the supporting conductive glass).

The photocurrent-potential curves were determined at room temperature, using 1.0 M KNO₃ as an electrolyte unless specified. Solution pH was adjusted with HClO₄. At least twenty minutes before use, the solution was equilibrated with N₂ (99.99%) or air.

A blue led (Phillips, LUXEON III, 3 W) was used as the illumination source. According to manufacturer's specifications, the led output has a Gaussian profile with a spectral half-width of 25 nm and a maximum at 470 nm. The incident photon flux impinging on the cell, *I*₀ = 8.4 × 10¹⁵ cm^{−2} s^{−1}, was estimated by chemical actinometry using the Reinecke salt.²⁸

Theoretical calculations

The geometry optimization and theoretical calculations of normal vibrational modes were carried out by using the Gaussian 03W²⁹ package of programs and employing the DFT formalism, using the 6-31G** basis set in the Becke three-parameter-Lee-Yang-Parr (B3LYP) exchange–correlation functional method. Simplified models consisting of an AC molecule attached to a single Ti atom and a set of water and hydroxyl ligands, as shown in Scheme 1, were used in order to calculate the Raman spectra. Vibrational frequencies were scaled by a factor of 0.98,³⁰ to yield calculated values in close agreement with experimental results. See ESI† for details.

Results and discussion

Alizarin complexone chemisorption on TiO₂ nanoparticles

The absorption spectrum of AC in the 50% water:ethanol mixture acidified at pH 1.5 shows a maxima at λ = 434 nm,

with $\varepsilon_{434} = 5200 \text{ M}^{-1} \text{ cm}^{-1}$. However, the addition of AC to a 4.5 mM solution of TiO_2 nanoparticles at pH 1.5 results in a wine-colored solution as shown in Fig. 1A. The appearance of the red-shifted absorption band is indicative of a strong bonding between AC and TiO_2 nanoparticles and suggests a perturbation of the electronic structure of the chromophore which is similar to that observed on deprotonation.^{17,18,31} From a Benesi-Hildebrand analysis of the adsorption data, we obtained the molar extinction coefficient of the complex at the absorption maxima, $\varepsilon_{480} = 11800 \text{ M}^{-1} \text{ cm}^{-1}$, and an estimation of the association constant for the binding of AC to TiO_2 , $K_{\text{BH}} = 1 \times 10^4 \text{ M}^{-1}$. Fig. 1B compares the molar extinction coefficient of the free dye and that of the AC@ TiO_2 complex. It should be stressed that both the red shift of the band and the increase in the absorption as a result of AC chemisorption closely resemble previous results obtained for the alizarin molecule.^{16–18} The strong interaction is not necessarily correlated with a direct charge injection mechanism (optical electron transfer). It has been demonstrated for A@ TiO_2 that despite the high affinity and the high injection rates, the visible band is better described as a localized $S_0 \rightarrow S_1$ excitation instead of direct charge-transfer absorption.³² Although further studies are needed for AC@ TiO_2 , it is reasonable to assume a similar result to that in the reference system.

Attempts to obtain AC modified nanostructured TiO_2 electrodes by dipping the films in water:ethanol solutions of AC at acidic pH resulted in very pale films. This result contrasts with the facile chemisorption observed under similar conditions in nanoparticulate sols. Thus, to promote binding we progressively dipped the films in more concentrated AC solutions and reduced

their H^+ content. Films of about 60% of transmittance at 480 nm could be obtained by equilibrating the films with concentrated AC solutions in pure ethanol. Fig. 1C shows the transmittance of the films supported on a conducting glass obtained before and after AC chemisorption and, for comparison, the spectrum of the free dye in ethanol. It is worthwhile to notice that the shoulder observed at 550 nm is indicative of partial ionization of the 2-OH bond. According to the reported pK values:²³ $\text{pK}_{\text{a}_1} = 2.40$ (–COOH), $\text{pK}_{\text{a}_2} = 5.54$ (2-OH), $\text{pK}_{\text{a}_3} = 10.07$ (–NHC) and $\text{pK}_{\text{a}_4} = 11.98$ (1-OH), AC is protonated at pH 1.5, and displays a negative charge above pH ~ 3.5 . It is worthwhile to say that $-\text{C}(\text{O})\text{O}-\text{H}$ dissociation of the carboxylic groups, which occurs near pH 2.4, does not produce any change in the absorption spectrum of AC. However, at pH values higher than 4.5, the ionization of the 2-OH group is accompanied with a decrease in the absorbance at 430 nm and the development of a new band having a maximum at 540 nm, as shown in Fig. 1D. Notice that at pH values close to 6.5, the complete dissociation of the 2-OH group becomes evident from the disappearance of the band at 430 nm and the full development of the band at 540 nm. It is apparent from these results that in the phenolate form, the absorption of the ligand is red shifted as compared to the protonated form, however, the spectra of AC complexes obtained in nanostructured films and nanoparticulate sols have nearly the same wavelength maxima (470 nm); the only difference being that the band is broader in the former case, *i.e.*, the observed width at half-height is 110 and 150 nm for suspended and supported complexes in TiO_2 nanoparticles, respectively. It is interesting to notice that the spectra of deprotonated and titania-bound AC show similar bathochromic changes of the low energy transition. However, the magnitude of this shift is smaller in the case of titania-bound AC, as the charge-induced perturbation of molecular orbitals is smaller than in the case of the deprotonated free dye.

The nature of the interactions between AC and TiO_2 nanoparticles was investigated by visible laser Raman spectroscopy.^{33–37} The Ar-ion laser line at 514 nm was used to photoexcite the charge-transfer complex, leading to an enhancement of the signal. The advantages of Raman spectroscopy over classical FTIR spectroscopy is that the resonance enhancement is restricted to the adsorbate involved in the charge transfer band, thus avoiding water interference.

The strongest features in the resonance Raman spectrum of AC chemisorbed in TiO_2 nanoparticles in solution or in the TiO_2 film are the ring stretches at 1445 and 1460 cm^{-1} . Less intense bands are observed at 1325 cm^{-1} (C–O stretch) and in the region between 1153 and 1200 cm^{-1} (C–H and C–O deformation bands), 1250 – 1300 cm^{-1} (C–O stretches coupled with ring stretches) and around 1590 cm^{-1} , which are assigned to skeletal modes of the benzene ring³⁸ (Fig. 2). The most important changes observed after AC binding are the loss of the in-plane OH bending and the broadening of the features related to the C–O band at 1180 cm^{-1} . It is clear from these results that this bond is involved in AC attachment to TiO_2 nanoparticles. On the other hand, the differences observed upon ligand chemisorption for alizarin and alizarin complexone molecules in solution (see ESI†) are strikingly

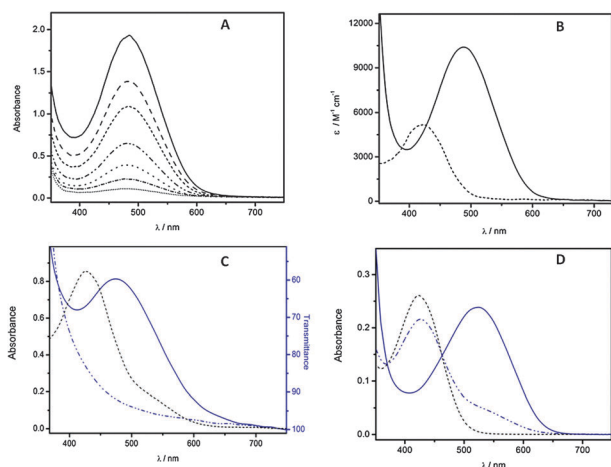


Fig. 1 (A) Changes in the absorption spectra recorded during the addition of variable amounts of alizarin complexone to a 4.5 mM TiO_2 sol. Final AC concentrations are from bottom to top: 5.6; 17; 34; 56; 84; 112.5 and 170 μM . (B) Molar extinction coefficient of free alizarin complexone (dash-dotted line) and the AC@ TiO_2 complex (solid line) both in 50% ethanol:water at pH 1.5. (C) Absorbance of 0.16 mM AC solution in ethanol (dashed line, left axis); and transmittance of the nanocrystalline titanium dioxide electrodes before (dash-dotted line, right axis) and after chemisorption of the dye (solid line, right axis). (D) Absorption spectra of 0.05 mM free alizarin complexone in 50% ethanol:water solutions at different pH values: 1.5 (dashed line), 4.5 (dash-dotted line) and 6.5 (solid line).

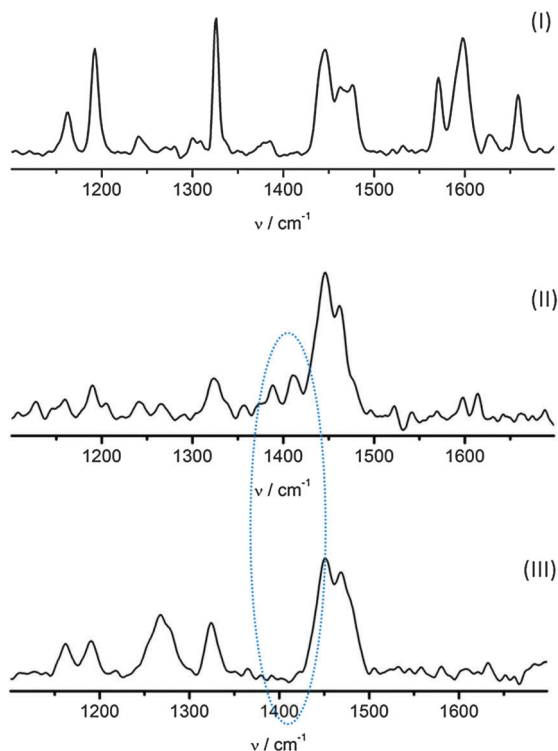


Fig. 2 SERS spectra of: free AC (I); AC@TiO₂ complexes at pH 1.5 ([TiO₂] = 30 mM; [AC] = 0.9 mM) (II); and AC@TiO₂ complexes obtained after dipping the TiO₂ films in ethanolic solutions of the ligand (III). Laser excitation wavelength: 514 nm.

similar. Based on the above experimental evidence and recent theoretical studies on related systems,³¹ we considered the possibility that AC also binds to TiO₂ through the OH groups as other enediol (*i.e.*, dopamine, catechol) molecules.^{19,36,39}

To further analyze this point we performed quantum chemical calculations considering that the attachment of AC to TiO₂ occurs through (a) the catechol moiety, (b) the (methylimino) diacetate and the 2-OH groups and (c) the 9-carbonyl and 1-OH groups. A summary of the most relevant results is presented in ESI.† It should be emphasized that these simplified models do not intend to represent the actual surface of TiO₂, but only to provide a basis for the discussion of the differences in the vibrational frequencies of the proposed binding modes. However, these minimalistic models are frequently employed to reproduce the basic spectral features of related systems.⁴⁰ According to the theoretical predictions both (a) and (b) cases seem to be compatible with the experimental results. However, the calculated Raman spectra for structure (a) show the presence of the bands at 1380 and 1410 cm⁻¹ assigned to skeletal ring modes coupled to C–O stretching, which are absent in the theoretical prediction for structure (b). This difference is also apparent for the AC@TiO₂ complexes obtained in aqueous and nanostructured films shown in Fig. 2, and seems to favor the prevalence of structure (a) over (b) for the complexes formed upon absorption of complexone in a sol of TiO₂ nanoparticles at pH 1.5.

Attachment of metal-alizarin complexone complexes to TiO₂ nanoparticles

As already mentioned in the Introduction we were interested in determining whether the various functionalities present in AC may provide a basis for the design of more complex nanostructures with distinctive photoelectrochemical behaviour.

The simultaneous attachment of alizarin complexone to Fe(II) and titanium dioxide has been previously analyzed by Jayaweera²¹ and coworkers. In their study, pre-manufactured AC@TiO₂ films were dipped in a Fe(II) solution. Based on the analysis of the FTIR spectra of the AC@TiO₂ films before and after Fe(II) chemisorption, they concluded that iron binding to AC@TiO₂ films occurs through the adjacent 9-C=O and 1-OH bonds.

To achieve a better control of surface coverage we used a different approach which apparently leads to distinct results. *First*, a stoichiometric tridentate complex [Fe^{II}-AC] was formed upon mixing 1 mM solutions of AC and Fe(II) ions. The spectrum of this complex, shown in the upper part of Fig. 3, has a maximum at 455 nm. *Then*, to obtain the modified electrodes, the TiO₂ films were dipped in the [Fe^{II}-AC] solution. Chemisorption of the complex becomes apparent by the coloration of the films ($\lambda_{\text{max}} = 480$ nm) and the broadening of the C–O band at 1100 cm⁻¹ in comparison with the Raman spectra obtained for AC@TiO₂ electrodes, as shown in Fig. 3. Based on the high stability of the M-AC complexes we propose that [Fe^{II}-AC] conserves its tridentate structure and binds to TiO₂ nanoparticles through the 9-C=O and 1-OH groups, see the scheme in the same figure. A similar six-membered chelate type complex has been found for quinizarin,⁴¹ a positional isomer of alizarin.

The proposed structure for [Fe^{II}-AC]@TiO₂ is also supported by the theoretical Raman calculations which show, as experimentally observed, the enhancement of the band at 1100 cm⁻¹.

Photocurrent determinations as a function of the applied potential

AC@TiO₂ films. Fig. 4 shows a typical *j*-*V* curve obtained under interrupted visible illumination of the working electrode at $\lambda = 470 \pm 25$ nm, scanning the applied potential from 400 to -400 mV at 1 mV s⁻¹. Sign reversal is observed nearby -90 mV at pH 6.5 in air saturated KNO₃ solutions.

The existence of anodic photocurrents is explained by the usual mechanism: after visible irradiation, the excited state of the dye injects an electron into the conduction band of the semiconductor. The positive current is then accounted by the fraction of the injected charges that escape recombination and manages to percolate through the nanoporous film. However, the development of negative photocurrents requires a charge flow in the opposite direction, *i.e.*, an electron discharge at the working electrode. Photocathodic currents have previously been found for alizarin¹⁶ and carminic acid¹⁵ attached to nanostructured TiO₂ films. In both cases the generation of negative currents has been rationalized by the involvement of the reductive excited state of the ligand acting as an intermediate in oxygen reduction.

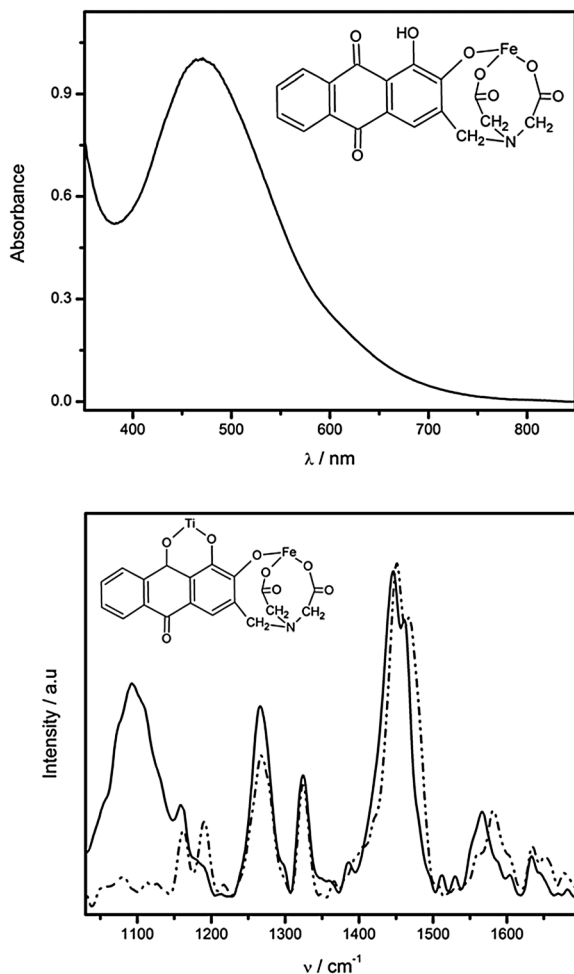


Fig. 3 Upper: the absorption spectrum and structure of the tridentate $\text{Fe}^{\text{II}}\text{-AC}$ complex. Lower: comparison between SERS spectra of AC@TiO_2 film (dash-dotted line) and $[\text{Fe}^{\text{II}}\text{AC}]\text{@TiO}_2$ film (solid line). Laser excitation wavelength: 514 nm. A schematic representation of the proposed $[\text{Fe}^{\text{II}}\text{AC}]\text{@TiO}_2$ structure is also shown, see text.

However, it has been recognized that this mechanism requires an efficient charge transport through the semiconductor in the interband gap region. Since at potentials more positive than the *flatband*, the Fermi level of the ITO electrode lies below the bottom of the conduction band of TiO_2 particles, electron transport should involve charge hopping between the ligand molecules and/or between surface states through the TiO_2 matrix, from the ITO to the electrolyte solution.¹⁶ Based on our previous detailed study,¹⁶ as well as the fact that no photocurrents could be detected in the presence of AC in solution using a bare ITO electrode, neither by excitation of AC on Al_2O_3 films supported on the conductive glass, we postulate that electron transport is dominated by surface states.

To summarize, we show in Scheme 2 the energy levels and the electron transfer pathway at negative bias, indicating that electrons from the ITO are transported through the TiO_2 layer by surface states before being captured in the excited state of the AC radical anion and discharged in the electrolyte solution.

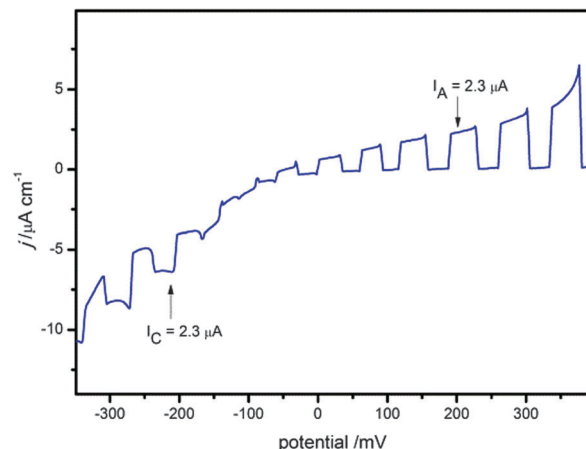


Fig. 4 Photocurrent–voltage curve obtained under interrupted illumination of the AC@TiO_2 system obtained during +400 to –400 mV scans at 1 mV s^{-1} . The curves were obtained in O_2 saturated 1.0 M KNO_3 solution at pH 6.5. Irradiation conditions, $\lambda = 470 \pm 25 \text{ nm}$; incident photons, $8.4 \times 10^{15} \text{ cm}^{-2} \text{ s}^{-1}$; film absorbance, 0.3. The potential is given vs. Ag/AgCl .

$[\text{Fe}^{\text{II}}\text{AC}]\text{@TiO}_2$ and $[\text{Fe}^{\text{III}}\text{AC}]\text{@TiO}_2$ films. The UV-Vis spectra of $[\text{Fe}^{\text{II}}\text{AC}]\text{@TiO}_2$ and AC@TiO_2 films were nearly identical (Fig. 5), thus, the excitation wavelength was also set at $\lambda = 470 \pm 25 \text{ nm}$.

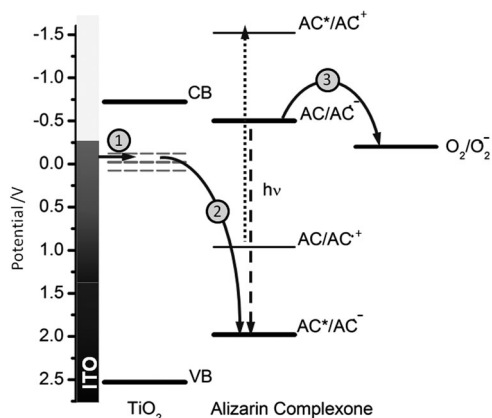
As shown in Fig. 6, $[\text{Fe}^{\text{II}}\text{AC}]\text{@TiO}_2$ electrodes always display anodic photocurrents, between 400 and –450 mV.

Detailed studies of the electrochemical behavior of AC and various M-AC complexes have shown that $E_{\text{red}}(\text{AC}/\text{ACH}_2)$ is not affected by metal complexation,^{42,43} thus, we postulate that the lack of cathodic currents observed for $[\text{Fe}^{\text{II}}\text{AC}]\text{@TiO}_2$ at variance with the results observed for AC@TiO_2 is directly correlated with the $\text{C}=\text{O}$ attachment to surface titanium atoms.

To verify our hypothesis we modified the nanostructured TiO_2 films with quinizarin, which as already mentioned binds to titanium dioxide through the 9- $\text{C}=\text{O}$ and 1-OH adjacent groups, and is supposed to have similar redox properties to alizarin.⁴⁰

By irradiating the charge transfer band of the Q@TiO_2 complex, see Fig. 7, we detected only anodic photocurrents. This is in line with our assumption that the binding of the quinone moiety to a Ti^{IV} centre at the TiO_2 surface prevents electron transfer from the conduction band to the ligand and, ultimately, oxygen reduction.

For completion, the tridentate complex of ferric ions with AC was used to prepare modified TiO_2 photoelectrodes. It is interesting to note that when $[\text{Fe}^{\text{III}}\text{AC}]\text{@TiO}_2$ films are used as working electrodes a sign reversal at –100 mV is observed (Fig. 6). The origin of the negative currents may be traced to the reduction of $\text{Fe}(\text{III})$ ions. Consistent with this proposal we observed that after prolonged irradiation at 470 nm the $[\text{Fe}^{\text{II}}\text{AC}]\text{@TiO}_2$ film oxidizes to $[\text{Fe}^{\text{III}}\text{AC}]\text{@TiO}_2$ and, afterwards, cathodic currents could be detected. However, bonding geometry seems to be of crucial importance, as AC metal complexes which are not electron acceptors behave like quinizarin. Interaction of the anion radicals with metal ions may stabilize them due to the



Scheme 2 Cathodic photocurrent is generated at negative bias. The proposed mechanism involves electron transport through surface states (1), followed by electron capture by the excited state of the AC radical ion (2), and oxygen reduction at the semiconductor–electrolyte interface (3). The potential is given vs. Ag/AgCl at pH 7. Dotted and dashed lines indicate, respectively, the generation of the excited radical cation and anion by visible irradiation from their corresponding ground states.

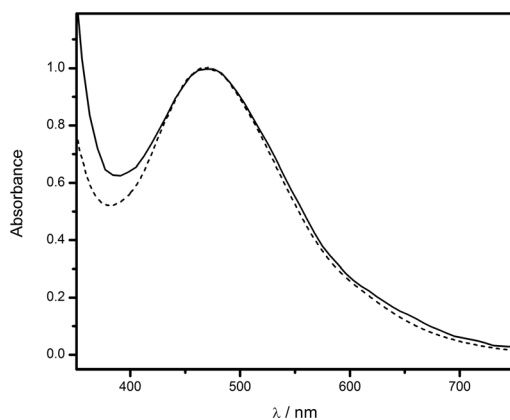


Fig. 5 Comparison between the normalized spectra of AC@TiO₂ (dashed line) and [Fe^{II}]AC@TiO₂ films (solid line).

formation of valence tautomers (especially with high-valent ions, e.g. Ti⁴⁺) and thus hamper their reaction with molecular oxygen.^{44,45} Therefore we can postulate that the central ring of the dye, with two unbound carbonyl groups is necessary for efficient oxygen reduction at the electrode surface.

Summary and conclusions

In summary, we have shown that AC is an interesting ligand for the design of nanostructured TiO₂ photoelectrodes showing the PEPS phenomenon. The basic framework provided by the alizarin ring retains the two redox-active quinoid fragments, the 9,10-dioxo and the 1,2-catechol-like fragment which may act as electron acceptor and electron-donor groups, respectively. Additionally, the (methylimino) diacetate group affords a moiety for metal chelation. The irreversible nature of AC metal complexes serves to redirect TiO₂ binding, *i.e.*, attachment of

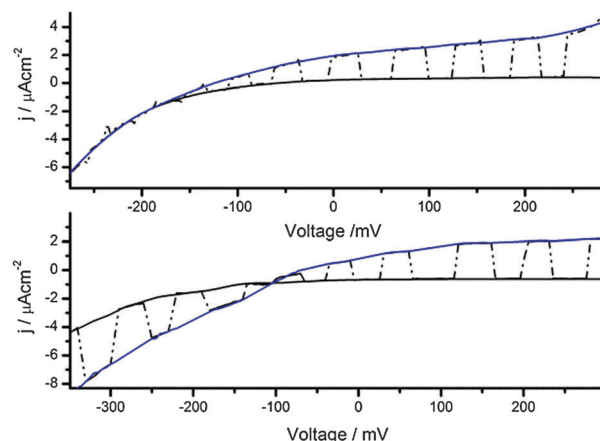


Fig. 6 Photocurrent–voltage curves obtained under interrupted illumination during +400 to −400 mV scans at 1 mV s^{−1} using [Fe^{II}]AC@TiO₂ (upper) and [Fe^{III}]AC@TiO₂ electrodes (lower). Other conditions are O₂ saturated atmosphere, electrolyte solution 1.0 M KNO₃ at pH 6.5. Irradiation wavelength 470 ± 25 nm; $I_0 = 8.4 \times 10^{15} \text{ cm}^{-2} \text{ s}^{-1}$. The potential is given vs. Ag/AgCl.

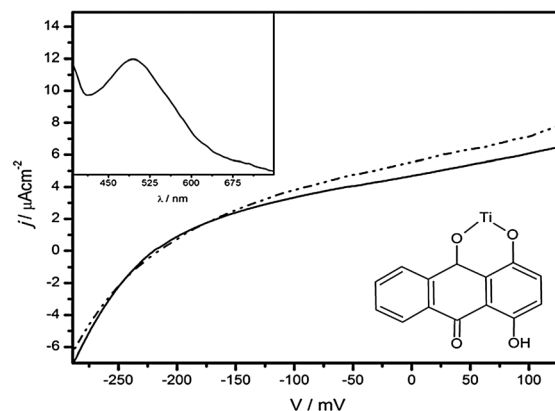


Fig. 7 Photocurrent–voltage curves obtained in the dark (solid line) and under illumination of Q@TiO₂ film (dash-dotted line); obtained during +300 to −300 mV scans at 1 mV s^{−1}. The curves were obtained in O₂ saturated 1.0 M KNO₃ solution at pH 6.5. Irradiation wavelength, $\lambda = 470 \pm 25 \text{ nm}$; $I_0 = 8.4 \times 10^{15} \text{ cm}^{-2} \text{ s}^{-1}$. The potential is given vs. Ag/AgCl. Inset: A spectrum of the Q@TiO₂ electrode, showing the low energy band. A simplified model for the chemical structure of Q@TiO₂ is also given, see text.

M-AC to TiO₂ films in these cases involves the C=O and OH groups at the 1,9 positions of the alizarin framework.

In AC@TiO₂ photoelectrodes, at negative bias, the electrons from the ITO are transported through the TiO₂ layer by surface states, captured by the surface dye molecules in the form of alizarin complexone anion radicals. These radicals are subsequently discharged to the electrolyte in reaction with dissolved oxygen solution accounting for the observed cathodic currents. By contrast, in [M-AC]@TiO₂ films the dye cannot support oxygen reduction because it is involved in TiO₂ binding. Thus, photocurrent polarity reversal for [M-AC]@TiO₂ photoelectrodes is only observed if the metal ion can be reduced. This is the reason why the PEPS effect can be observed in [Fe^{III}]AC@TiO₂ and not in [Fe^{II}]AC@TiO₂ electrodes. The current study

highlights the relevance of both geometric and electronic factors in the mechanism of the PEPS effect.

Acknowledgements

This work was financially supported by the University of Mar del Plata and the National Research Council of Argentina (CONICET), project PIP 319 and The National Science Centre (Poland) within contract UMO-2011/03/B/ST5/01495. YDI thanks CONICET for a postdoctoral fellowship.

References

- 1 K. Szaciłowski, *Chem. Rev.*, 2008, **108**, 3481.
- 2 S. Gaweda, R. Kowalik, P. Kwolek, W. Macyk, J. Mech, M. Oszejca, A. Podborska and K. Szaciłowski, *Isr. J. Chem.*, 2011, **51**, 36.
- 3 D. Chen and J. Li, *J. Phys. Chem. C*, 2010, **114**, 10478.
- 4 X. Lv, H. Chang and H. Zhang, *Opt. Commun.*, 2011, **284**, 4991.
- 5 M. F. Oszejca, K. L. McCall, N. Robertson and K. Szaciłowski, *J. Phys. Chem. C*, 2011, **115**, 12187.
- 6 A. N. Shipway, E. Katz and I. Willner, *ChemPhysChem*, 2000, **1**, 18.
- 7 F. Hollmann, A. Schmid and E. Steckhan, *Angew. Chem., Int. Ed.*, 2001, **40**, 154.
- 8 (a) Y. Liu, J. Li, B. Zhou, H. Chen, Z. Wang and W. Cai, *Chem. Commun.*, 2011, **47**, 10314; (b) Y. Liu, J. Li, B. Zhou, S. Lv, X. Li, H. Chen, Q. Chen and W. Cai, *Appl. Catal., B*, 2012, **111–112**, 485.
- 9 F. Davis, S. D. Collyer and S. P. J. Higson, *Top. Curr. Chem.*, 2005, **255**, 97.
- 10 A. Fujishima, X. Zhang and D. A. Tryk, *Surf. Sci. Rep.*, 2008, **63**, 512.
- 11 (a) M. Oszejca, P. Kwolek, J. Mech and K. Szaciłowski, *Curr. Phys. Chem.*, 2011, **1**, 242; (b) W. Macyk, K. Szaciłowski, G. Stochel, M. Buchalska, J. Kunciewicz and P. Łabuz, *Coord. Chem. Rev.*, 2010, **254**, 2687; (c) P. Kwolek, M. Oszejca and K. Szaciłowski, *Coord. Chem. Rev.*, 2012, **256**, 1706.
- 12 L. F. O. Furtado, A. D. P. Alexiou, L. Gongalves, H. E. Toma and K. Araki, *Angew. Chem., Int. Ed.*, 2006, **45**, 3143.
- 13 J. Zhou, L. Lin, L. Zhang and Z. Lin, *J. Phys. Chem. C*, 2011, **115**, 16828.
- 14 K. Szaciłowski, W. Macyk and G. Stochel, *J. Am. Chem. Soc.*, 2006, **128**, 4550.
- 15 S. Gaweda, G. Stochel and K. Szaciłowski, *J. Phys. Chem. C*, 2008, **112**, 19131.
- 16 Y. Di Iorio, H. B. Rodriguez, E. San Roman and M. A. Grela, *J. Phys. Chem. C*, 2010, **114**, 11515.
- 17 Y. Di Iorio, M. A. Brusa, A. Feldhoff and M. A. Grela, *ChemPhysChem*, 2009, **10**, 1077.
- 18 Y. Di Iorio, E. S. Roman, M. I. Litter and M. A. Grela, *J. Phys. Chem. C*, 2008, **112**, 16532.
- 19 (a) W. R. Duncan and O. V. Prezhdo, *J. Phys. Chem. B*, 2005, **109**, 365; (b) T. Rajh, L. X. Chen, K. Lukas, T. Liu, M. C. Thurnauer and D. M. Tiede, *J. Phys. Chem. B*, 2002, **106**, 10543.
- 20 E. Palomares, R. Vilar, A. Green and J. R. Durrant, *Adv. Funct. Mater.*, 2004, **14**, 111.
- 21 W. M. G. I. Priyadarshana and P. M. Jayaweera, *Colloids Surf., A*, 2009, **335**, 144.
- 22 H. Kunkely and A. Vogler, *Inorg. Chem. Commun.*, 2007, **10**, 355.
- 23 T. Yokoyama, K. Tashiro, T. Murao, A. Yanase, J. Nishimoto and M. Zenki, *Anal. Chim. Acta*, 1999, **398**, 75.
- 24 V. Y. Fain, V. G. Avakyan, B. E. Zaitsev and M. A. Ryabov, *Russ. J. Coord. Chem.*, 2004, **30**, 671.
- 25 S. H. Etaiw, R. M. Issa and N. B. El-Assy, *J. Inorg. Nucl. Chem.*, 1981, **43**, 303.
- 26 S. K. Ali, M. A. Khan and G. M. Bouet, *J. Chem. Soc. Pak.*, 2005, **27**, 109.
- 27 J. Zhang, A. B. P. Lever and W. J. Pietro, *Inorg. Chem.*, 1994, **33**, 1392.
- 28 E. E. Wegner and A. W. Adamson, *J. Am. Chem. Soc.*, 1966, **88**, 394.
- 29 M. J. Frisch, G. W. Trucks, H. B. Schlegel, G. E. Scuseria, M. A. Robb, J. R. Cheeseman, J. A. Montgomery, Jr., T. Vreven, K. N. Kudin, J. C. Burant, M. Millam, S. S. Iyengar, J. Tomasi, V. Barone, B. Mennucci, M. Cossi, G. Scalmani, N. Rega, G. A. Petersson, H. Nakatsuji, M. Hada, M. Ehara, K. Toyota, R. Fukuda, J. Hasegawa, M. Ishida, T. Nakajima, Y. Honda, O. Kitao, H. Nakai, M. Klene, X. Li, J. E. Knox, H. P. Hratchian, J. B. Cross, C. Adamo, J. Jaramillo, R. Gomperts, R. E. Stratmann, O. Yazyev, A. J. Austin, R. Cammi, C. Pomelli, J. W. Ochterski, P. Y. Ayala, K. Morokuma, G. A. Voth, P. Salvador, J. J. Dannenberg, V. G. Zakrzewski, S. Dapprich, A. D. Daniels, M. C. Strain, O. Farkas, D. K. Malick, A. D. Rabuck, K. Raghavachari, J. B. Foresman, J. V. Ortiz, Q. Cui, A. G. Baboul, S. Clifford, J. Cioslowski, B. B. Stefanov, G. Liu, A. Liashenko, P. Piskorz, I. Komaromi, R. L. Martin, D. J. Fox, T. Keith, M. A. Al-Laham, C. Y. Peng, A. Nanayakkara, M. Challacombe, P. M. W. Gill, B. Johnson, W. Chen, M. W. Wong, C. Gonzalez and J. A. Pople, *Gaussian 03, Revision A.1*, Gaussian, Inc., Pittsburgh, PA, 2003.
- 30 E. Kavitha, N. Sundaraganesan and S. Sebastian, *Indian J. Pure Appl. Phys.*, 2010, **48**, 20.
- 31 (a) O. V. Prezhdo, R. W. Duncan and V. V. Prezhdo, *Acc. Chem. Res.*, 2008, **41**, 339; (b) O. V. Prezhdo, W. R. Duncan and V. V. Prezhdo, *Prog. Surf. Sci.*, 2009, **84**, 30; (c) W. Stier and O. V. Prezhdo, *J. Phys. Chem. B*, 2002, **106**, 8047; (d) W. Stier and O. V. Prezhdo, *Isr. J. Chem.*, 2002, **42**, 213.
- 32 (a) R. Huber, S. Spörlein, J. E. Moser, M. Grätzel and J. Wachtveitl, *J. Phys. Chem. B*, 2000, **104**, 899; (b) R. Huber, J. E. Moser, M. Grätzel and J. Wachtveitl, *J. Phys. Chem. B*, 2002, **106**, 6494.
- 33 T. Lana-Villarreal, A. Rodes, J. M. Perez and R. Gomez, *J. Am. Chem. Soc.*, 2005, **127**, 12601.
- 34 K. E. Lee, M. A. Gomez, S. Elouatik and G. P. Demopoulos, *Langmuir*, 2010, **26**, 9575.
- 35 A. Musumeci, D. Gosztola, T. Schiller, N. M. Dimitrijevic, V. Mujica, D. Martin and T. Rajh, *J. Am. Chem. Soc.*, 2009, **131**, 6040.
- 36 P. Tarakeshwar, D. Finkelstein-Shapiro, S. J. Hurst, T. Rajh and V. Mujica, *J. Phys. Chem. C*, 2011, **115**, 8994.

- 37 S. J. Hurst, H. C. Fry, D. J. Gosztola and T. Rajh, *J. Phys. Chem. C*, 2011, **115**, 620.
- 38 L. C. T. Shoute and G. R. Loppnow, *J. Chem. Phys.*, 2002, **117**, 842.
- 39 T. Rajh, Z. Saponjic, J. Liu, N. M. Dimitrijevic, N. F. Scherer, M. Vega-Arroyo, P. Zapol, L. A. Curtiss and M. C. Thurnauer, *Nano Lett.*, 2004, **4**, 1017.
- 40 (a) R. Sánchez-de-Armas, J. Oviedo, M. A. San-Miguel and J. F. Sanz, *J. Phys. Chem. C*, 2011, **115**, 11293; (b) R. Sánchez-de-Armas, J. Oviedo, M. A. San-Miguel and J. F. Sanz, *Phys. Chem. Chem. Phys.*, 2011, **13**, 1506.
- 41 G. Ramakrishna, A. K. Singh, D. K. Palit and H. N. Ghosh, *J. Phys. Chem. B*, 2004, **108**, 4775.
- 42 J. Zhang, A. B. P. Lever and W. J. Pietro, *J. Electroanal. Chem.*, 1995, **385**, 191.
- 43 A. L. B. Marques, W. Li, E. P. Marques and J. Zhang, *Electrochim. Acta*, 2004, **49**, 879.
- 44 A. Dei, D. Gatteschi, C. Sangregorio and L. Sorace, *Acc. Chem. Res.*, 2004, **37**, 827.
- 45 J. A. Reingold, S. U. Son, S. B. Kim, C. A. Dullaghan, M. Oh, P. C. Frake, G. B. Carpenter and D. A. Sweigart, *Dalton Trans.*, 2006, 2385.